Synthesizing dispersion relations in a modulated tilted optical lattice

Jean Claude Garreau and Véronique Zehnlé
Université Lille, CNRS, UMR 8523 - PhLAM - Laboratoire de Physique des Lasers Atomes et Molécules, F-59000 Lille, France

(Received 22 July 2021; revised 3 January 2022; accepted 7 January 2022; published 25 January 2022)

Dispersion relations are fundamental characteristics of the dynamics of quantum and wave systems. In this work we introduce a simple technique to generate a large variety of dispersion relations in a modulated tilted lattice. The technique is illustrated by important examples: the Dirac, Bogoliubov, and Landau dispersion relations (the latter exhibiting the roton and the maxon). We show that adding a slow temporal phase shift to the lattice modulation allows one to reconstruct the dispersion relation from dynamical quantities. Finally, we generalize the technique to higher dimensions and generate graphenelike Dirac points and flat bands in two dimensions.

DOI: 10.1103/PhysRevA.105.013318

I. INTRODUCTION

Dispersion relations, connecting the energy to the momentum, $E = E(\boldsymbol{p})$, of a quantum particle, or the frequency to the wave number $\omega = \omega(\boldsymbol{k})$ of a wave, are a fundamental concept in many domains of physics. For example, relativistic particles are characterized by the Einstein's dispersion relation $E^2 = p^2c^2 + m^2c^4$, crystalline solids by their bands $E = E(\boldsymbol{q})$ (with $\boldsymbol{q}$ the quasimomentum), and superfluidity by Landau's dispersion relation, presenting exotic features like the *maxon* and the *roton* [1–3]. Dispersion relations provide a great deal of information on the physics of a system.

Recent developments both in condensed-matter and ultracold-atom systems have generated the concept of a "quantum simulators." Devising, for instance, a system displaying a given dispersion relation provides information several aspects of the physics of other systems exhibiting the same dispersion relation. Ultracold atoms in optical lattices or trapped ions have proved to be among the most clean and flexible systems in physics, both theoretically and experimentally. Optical lattices can mimic an almost perfect lattice (no phonons, controllable decoherence, etc.) and make it easy to create low-dimensional systems. Moreover, being formed by the interference of laser beams, they can be "engineered" in many ways, i.e., one can create a wealth of different lattices. A few nonexhaustive examples are kagome [4], Lieb [5–7], quasiperiodic [8], and disordered lattices [9]. They can also be easily modulated in time, producing, notably, oscillating [10] or accelerated lattices [11,12]. These properties make such systems an outstanding platform to the realization of analog quantum simulators. In many cases one can construct a given Hamiltonian from its building blocks, e.g., Bose- and Fermi-Hubbard's [13–15], Anderson's [8,9,16,17], and Dirac's [18–22] Hamiltonians, bringing new light into many aspects of their physics, notably the Mott transition [14], the Anderson localization and transition [17,23–25], Bloch oscillations and Wannier-Stark ladders [11,12], or Klein tunneling [26,27]. Proposals for manipulating dispersion relations by applying temporal modulations in lattices are discussed in [28–30] and references therein.

In the present work we present a simple one-dimensional system able to "synthesize" several types of dispersion relations that we illustrate with important examples. An original technique allowing the direct detection of these dispersion relations is also proposed. In the last part we generalize the synthesis of dispersion relations to higher dimensions, illustrated by the generation of graphenelike Dirac cones and Lieb lattices (displaying a flat band) in two dimensions (2D).

II. SYNTHESIZING DISPERSION RELATIONS IN ONE-DIMENSIONAL WANNIER-STARK OPTICAL LATTICES

Our present model is based on the framework introduced in Ref. [21] and further developed in [22]. Ultracold atoms are placed in the interference pattern of counterpropagating laser beams, which generates a sinusoidal potential, proportional to the atom-laser coupling, acting on the center-of-mass degree of freedom of the atoms [31]. If the atom's de Broglie wavelength is comparable to the lattice constant $\mathsf{a} = \lambda_L/2$ ($\lambda_L = 2\pi/k_L$ is the radiation wavelength) [32], the system is in the quantum regime, a condition easily realized for temperatures of the order of a few μK. A linear shift of the frequency produces a quadratic displacement of the nodes of the standing wave [11,12,33] and the resulting inertial constant force creates a tilt, that is, a potential of the form $\mathsf{V}_{\rm ws}(\mathsf{x}) = -\mathsf{V}_1\cos(2k_L\mathsf{x}) + \mathsf{F}\mathsf{x}$, with V_1 proportional to the radiation intensity and F (constant) proportional to the frequency chirp [34]. The atomic cloud density is assumed low enough that atomic interactions are negligible.

A set of dimensionless units is obtained by measuring space in units of a, energy in units of the so-called atom's recoil energy $\mathsf{E}_R = \hbar^2k_L^2/2M = \hbar\omega_R$, and time in units of ω_R^{-1} (M is the atom's mass). This leads to the dimensionless Hamiltonian

$$H_0 = \frac{p^2}{2m^*} - V_0\cos(2\pi x) + Fx, \tag{1}$$

where $m^* = \pi^2/2$, $F = \mathsf{F}\mathsf{a}/\mathsf{E}_R$, and $V_0 = \mathsf{V}_1/\mathsf{E}_R$ are dimensionless quantities and Planck's constant is 1.

The properties of such a system, that we shall call a *tilted lattice*, are well known [35–41]. In short, this system is invariant under discrete spatial translations corresponding to an integer multiple n of the lattice step ($a = 1$ in dimensionless units) provided the energy is also shifted of $n\omega_B$ ($n\omega_B$ is the shift amount) where $\omega_B \equiv F$ is the so-called Bloch frequency ($= |\mathsf{F}|\mathsf{a}/\hbar$ in dimensioned units). In the following, n denotes the site index corresponding to potential minima localized at the position $x = n$. The symmetry of the system implies that the eigenfunctions (called Wannier-Stark states) are invariant under a translation of an integer number of lattice steps, i.e., $\varphi_n^{(\ell)}(x) = \varphi_0^{(\ell)}(x-n)$, with the corresponding eigenenergies $E_n^{(\ell)} = E_0^{(\ell)} + n\omega_B$, thus forming (depending on parameters V_0 and F) different ladders (labeled by ℓ) of levels separated by the constant step ω_B and characterized by a ground energy shift $E_0^{(\ell)}$. In what follows we will mainly consider potential parameters allowing two ladders ($\ell = g, e$) of localized "ground" and "excited" eigenstates, that is, there are two states localized at each site n, $\varphi_n^{(g)}(x)$ and $\varphi_n^{(e)}(x)$, separated by an energy shift $\Delta = E_0^{(e)} - E_0^{(g)}$. Other eigenstates of H_0, localized or belonging to the continuum, are assumed to be irrelevant for the system's dynamics, as explained below.

Controllable dynamics can be induced in such systems by external modulations of the parameters V_0 or F at frequencies close to resonances, i.e., close to Δ or to multiples of ω_B. We thus add to H_0 a time-dependent potential

$$H_1(t) = f(t)V(x), \tag{2}$$

where $V(x) = \cos(2\pi x)$. Using this flexibility, the feasibility of models reproducing the Dirac equation (hence the Dirac dispersion relation) has been demonstrated in Refs. [21,22].

The driving $f(t)$ has the general form

$$f(t) = \sum_{j,q} A_{j,q} e^{ij\omega_B t} e^{iq\Delta t}, \tag{3}$$

with $j \in \mathbb{Z}$, $q = 0, \pm 1$, and $A_{j,q} = A^*_{-j,-q}$ (reality condition). For given integers j the modulation resonantly couples states centered in sites separated by j lattice steps. If $q = 0$, one couples states $\varphi_n^{(\ell)}$ and $\varphi_{n+j}^{(\ell)}$ belonging to the same ladder ℓ (*intraladder* coupling). *Interladder* couplings between states $\varphi_n^{(g)}$ and $\varphi_{n+j}^{(e)}$ are obtained for $q = 1$, or $\varphi_n^{(e)}$ and $\varphi_{n+j}^{(g)}$ for $q = -1$.

With the above provisions, the general solution for the system can be developed in the Wannier-Stark basis restricted to the subspace spanned by the ground and first excited ladder

$$\Psi(x,t) = \sum_n \left[c_n(t) e^{-in\omega_B t} \varphi_n^{(g)}(x) + d_n(t) e^{-i(n\omega_B + \Delta)t} \varphi_n^{(e)}(x) \right] \tag{4}$$

a form that holds if modulation amplitudes in $f(t)$ are low enough to avoid projection on other eigenstates of the Hamiltonian H_0.

Plugging this form into the Schrödinger equation for $H_0 + H_1(t)$, one obtains a set of coupled differential equations for the amplitudes $c_n(t)$ and $d_n(t)$ (for details of this calculation, see the Appendix of Ref. [21]), which reads

$$i\frac{d}{dt}\begin{pmatrix} c_n(t) \\ d_n(t) \end{pmatrix} = \sum_{r\in\mathbb{Z}} \begin{pmatrix} T_r^{(gg)} & T_r^{(ge)} \\ T_r^{(eg)} & T_r^{(ee)} \end{pmatrix} \begin{pmatrix} c_{n+r}(t) \\ d_{n+r}(t) \end{pmatrix} \tag{5}$$

with coupling amplitudes between sites n and $n + r$ [42]:

$$\begin{aligned} T_r^{(gg)} &= A_{r,0} \langle \varphi_0^{(g)} | V | \varphi_r^{(g)} \rangle \\ T_r^{(ee)} &= A_{r,0} \langle \varphi_0^{(e)} | V | \varphi_r^{(e)} \rangle \\ T_r^{(ge)} &= A_{r,1} \langle \varphi_0^{(g)} | V | \varphi_r^{(e)} \rangle \\ T_r^{(eg)} &= A_{r,-1} \langle \varphi_0^{(e)} | V | \varphi_r^{(g)} \rangle. \end{aligned} \tag{6}$$

In the momentum representation the corresponding amplitudes $\tilde{c}(k,t) = \sum_n c_n(t) \exp(-ikn)$ (with analogous expressions for d_n) are governed by only *two* coupled equations:

$$i\frac{d}{dt}\begin{pmatrix} \tilde{c}(k,t) \\ \tilde{d}(k,t) \end{pmatrix} = \begin{pmatrix} F_g(k) & F(k) \\ F^*(k) & F_e(k) \end{pmatrix} \begin{pmatrix} \tilde{c}(k,t) \\ \tilde{d}(k,t) \end{pmatrix} \tag{7}$$

where

$$F_\ell(k) = \sum_{r=-\infty}^{\infty} T_r^{(\ell\ell)} e^{ikr} \tag{8}$$

with $\ell = \{g, e\}$, and

$$F(k) = \sum_{r=-\infty}^{\infty} T_r^{(ge)} e^{ikr}. \tag{9}$$

The functions $F_\ell(k)$ and $F(k)$ are Fourier series whose coefficients are proportional to the overlap integrals $T_r^{(\ell,\ell')}$ of the wave functions centered at positions separated by r sites but *are controlled by the modulation coefficients* $A_{j,q}$ [see Eqs. (6)].

Equations (7) define an effective Hamiltonian for a two-level-like system whose eigenvalues determine the dispersion relation $\omega(k)$:

$$[\omega(k) - F_g(k)][\omega(k) - F_e(k)] = |F(k)|^2. \tag{10}$$

This dispersion relation is 2π periodic and is conventionally defined in the interval $k \in (-\pi, \pi]$. Equation (10) is the basis of our technique for synthesizing dispersion relations: Specifying a given dispersion relation amounts to define the functions $F_g(k)$, $F_e(k)$, and $F(k)$, and from Eqs. (8) and (9), this sets conditions on the amplitudes $T_r^{(\ell,\ell')}$, which allows one, with the help of Eqs. (6), to determine modulation parameters $A_{j,q}$ that must be used in the modulation term $H_1(t)$. Examples discussed in Sec. III illustrate how a desired dispersion relation can be obtained to a very good approximation.

III. APPLICATIONS

A. Dirac cone

A linear dispersion relation $\omega(k) = \pm c|k|$, also called Dirac cone (corresponding to a Dirac particle of zero mass), can be obtained from Eq. (10) with $F_g(k) = F_e(k) = 0$ and $F(k) = c|k|$. This implies $T_r^{(g,g)} = T_r^{(e,e)} = 0$, that is, no intraladder couplings, and interladder couplings given by

Eq. (9). As the Fourier series of the function $|k|$ is

$$|k| = \left[\frac{\pi}{2} - \frac{4}{\pi}\sum_{r=1}^{\infty}\frac{\cos(rk)}{r^2}\right],$$

one must have

$$\sum_r T_r^{(g,e)} e^{ikr} = c|k| = c\left[\frac{\pi}{2} - \frac{4}{\pi}\sum_r \frac{\cos(rk)}{r^2}\right],$$

which, from Eq. (6), gives the modulation amplitudes

$$A_{0,1}\langle\varphi_0^{(g)}|V|\varphi_0^{(e)}\rangle = c\frac{\pi}{2} \qquad (11)$$

and

$$A_{r,1}\langle\varphi_0^{(g)}|V|\varphi_r^{(e)}\rangle = \frac{c}{\pi r^2}[\cos(r\pi) - 1] \qquad r > 0.$$

The dispersion relation is thus synthesized by applying a modulation given by Eq. (3) with coefficients

$$A_{r,1} = \frac{c\pi}{2}\langle\varphi_0^{(g)}|V|\varphi_0^{(e)}\rangle^{-1}\delta_{r,0} + \frac{c}{\pi r^2}\{\cos(r\pi) - 1\}\langle\varphi_0^{(g)}|V|\varphi_r^{(e)}\rangle^{-1}(1 - \delta_{r0}).$$

Experimentally, this modulation can be easily created by an arbitrary-wave generator. The overlap integrals $\langle\varphi_0^{(g)}|V|\varphi_r^{(e)}\rangle$ depend on the lattice parameters V_0 and F and go to zero rather fast with the site distance r, implying that the modulation amplitude at higher frequencies must increase rapidly, eventually breaking the slow modulation condition implied by Eq. (4). Fortunately, for typical lattice parameters, keeping only $r \leqslant 3$ terms yet gives a rather good approximation of a Dirac cone, as shown Fig. 1 (top), except at the tip of the cone at $k = 0$ which needs higher harmonics to be well reproduced.

A way to overcome this limitation is to include in Eq. (11) a frequency offset parameter b such that $\omega(k) = \pm c(|k| + b)$, which is readily done by setting

$$A_{0,1} = c\left(b + \frac{\pi}{2}\right)\langle\varphi_0^{(g)}|V|\varphi_0^{(g)}\rangle^{-1}.$$

The parameter b controls the gap between the two half-cones: If $b > 0$ a gap is opened, and if $b < 0$ one obtains two intersecting Dirac cones. Figure 1 (bottom) illustrates this case for $b = -1$ and shows perfect linear behavior in the vicinity of the Dirac points whose position $k = \pm b$ is controlled by the applied modulation. We have thus obtained a flexible way to generate Dirac-cone-type dispersion relations, allowing one to open a gap or to merge the cones.

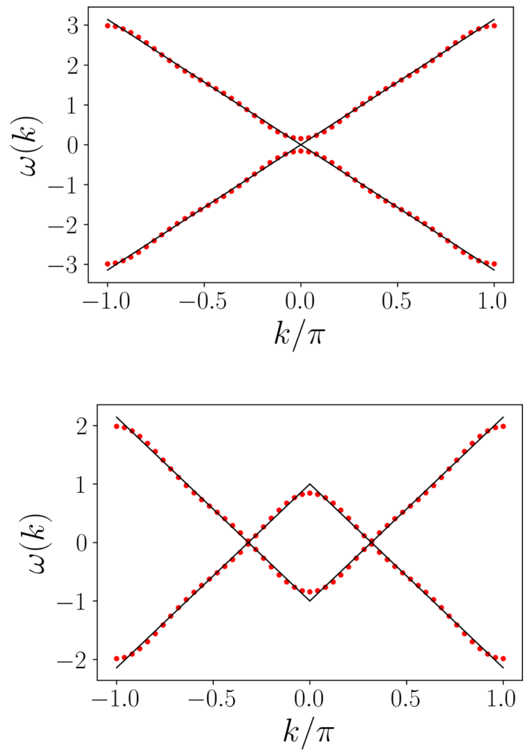

FIG. 1. Linear dispersion relation. *Top*: Dirac cone ($c = 1$). *Bottom*: Intersecting Dirac cones ($c = 1, b = -1$). Only terms $0 \leqslant r \leqslant 3$ were kept in the Fourier series (red circles). The analytical expressions are shown for comparison (black solid lines).

B. The superfluid dispersion relation, the roton and the maxon

Superfluidity is a purely quantum behavior appearing notably in liquid helium and quantum atomic gases. Its simplest mathematical treatment relies on the Bogoliubov correction to the mean-field Gross-Pitaevskii equation [3,31,43], which leads to the well-known Bogoliubov dispersion relation

$$\omega(k) = \sqrt{\frac{k^2}{2M}\left(\frac{\hbar^2 k^2}{2M} + 2gn\right)}, \qquad (12)$$

where M is the atom mass, g a parameter characterizing the binary atomic interaction in the Gross-Pitaevskii equation, and n the atomic density (the approximation is valid in the limit of low density and temperature). This dispersion is characterized by a "phononic," i.e., linear $\omega(k) \propto k$ dependence at small k ($k \ll \sqrt{gnM}/\hbar$) and a "free particle" part $\omega(k) \propto k^2$ at large k.

Following the same ideas as in the preceding section, Eq. (12) can be obtained from the general form of the dispersion relation with $F_g(k) = F_e(k) = 0$ and

$$F(k) = c(|k| + \alpha k^2), \qquad (13)$$

where α is an imaginary number ($\alpha = i|\alpha|$), leading, through Eq. (10), to the desired dispersion

$$\omega(k) = c\sqrt{k^2(1 + |\alpha|^2 k^2)}. \qquad (14)$$

Beyond the Bogoliubov approach, phenomenological arguments by Landau [1] concerning the superfluidity of the strongly interacting liquid ^{4}He supported the existence in the dispersion relation of a minimum $\omega(k_r)$ at some k_r, called the *roton* [44] which, by continuity, implies the existence of a maximum $\omega(k_m)$ with $k_m < k_r$, called the *maxon*. Roton and maxon features have recently been observed experimentally using a Bose-Einstein condensate in a modulated flat lattice [45], in erbium condensates with interactions controlled by Feshbach resonances [46,47], and in acoustic metamaterials [48].

A dispersion relation presenting a roton and maxon can be synthesized by choosing α as a *complex* number, leading to

$$\omega(k) = c\sqrt{k^2(1 + (\alpha + \alpha^*)|k| + |\alpha|^2 k^2)}. \qquad (15)$$

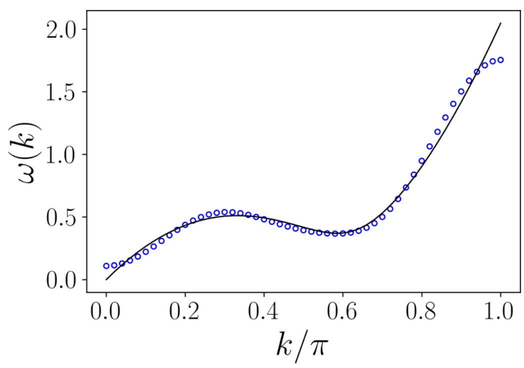

FIG. 2. Synthetic dispersion relation displaying a maxon and a roton, generated by the Fourier series Eq. (16) (blue circles), restricted to $|r| \leqslant 3$, compared to Eq. (15) with parameters $c = 1$ and $\alpha = -0.5 + 0.1i$ (black solid line).

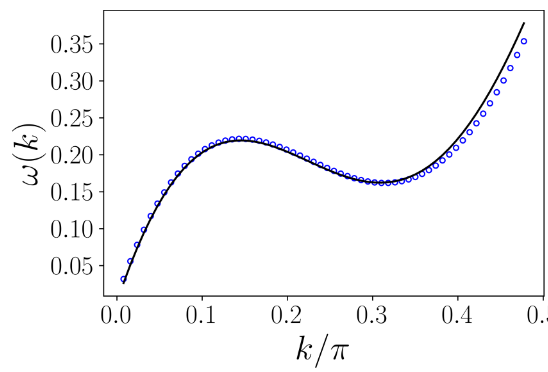

FIG. 3. Detecting the dispersion relation. The solid black line dispersion relation is obtained from $\omega(k) = F_g[k + \phi(t)]$ with $F_g(k) = -0.81[1 - \cos(2k)] - 0.5\sin(2k) + 2\sin k$ and $F_e = F = 0$. The blue circles show the average wave-packet position $\langle X\rangle(t)$ (with an adjusted vertical scale factor) and the phase-shift ratio $\gamma = \pi \times 10^{-4}\omega_B$.

Equation (9) then leads to

$$T_r^{(ge)} = A_{r,1}\langle\varphi_0^g|V|\varphi_r^e\rangle = \frac{c}{\pi}\int_0^\pi \cos(rk)(|k| + \alpha k^2),$$

from which we obtain the modulation amplitudes

$$A_{r,1} = c\left(\frac{\pi}{2} + \alpha\frac{\pi^2}{3}\right)\langle\varphi_0^{(g)}|V|\varphi_0^{(e)}\rangle^{-1}\delta_{r0} + \frac{c}{\pi r^2}[(2\pi\alpha+1)\cos(r\pi) - 1]\langle\varphi_0^{(g)}|V|\varphi_r^{(e)}\rangle^{-1}(1-\delta_{r0}). \quad (16)$$

The fact that $|A_{r,1}| \propto r^{-2}$ (for $r \neq 0$) implies that the series has a rather fast convergence, and thus that only a few terms suffice to give a good approximation of the desired dispersion relation. Figure 2 shows the resulting Bogoliubov dispersion relation with the *roton-maxon* features obtained for $\alpha = -0.5 + 0.1i$, compared to Eq. (15).

C. Scanning the dispersion relation

A natural question is how to obtain experimental information on the shape of the dispersion relation. We show below that this can be done by preparing an initial wave packet and monitoring its average position $\langle X\rangle(t)$ in the modulated lattice while applying a slow phase shift to the modulation Eq. (3). We thus use a generalized modulation form $\sum_j A_{j,q}\exp(i[j(\omega_B t + \phi(t)) + q\Delta t])$, where $\phi(t)$ is an arbitrary time-dependent phase. All the developments of Sec. II remain valid, except that for a slow variation of $\phi(t)$, the amplitudes become $A_{j,q}\exp(ij\phi(t))$. Equations (6) show that the phase modulation $\phi(t)$ is then imprinted in the coupling coefficients $T_r^{(\ell,\ell')}$, which finally results in shifting $k \to k(t) = k + \phi(t)$ in Eqs. (8) and (9). Changing the phase ϕ turns out to be equivalent to changing k [49], resulting in slowly varying functions $F(k(t))$ and $F_\ell(k(t))$ and thus $\omega(k(t))$.

We illustrate this idea in the simple case of an intraladder model with only the ground ladder $\ell = 0$ [i.e., $q = 0$ in Eq. (2)]. In this case we have $\omega(k) = F_g[k + \phi(t)]$, and a slow linear phase shift $\phi = \gamma t$ ($\gamma \ll \omega_B$) results in $\langle X\rangle(t) = \omega(k)|_{k=k(t)}/\gamma$ (see Appendix). We choose here the example of an analytical dispersion relation

$$\omega(k) = a[1 - \cos(2k)] + b\sin(2k) + c\sin k, \quad (17)$$

which exhibits a rotonlike behavior as shown in Fig. 3 (full black line). We performed a numerical simulation of the full Schrödinger equation corresponding to the Hamiltonian $H = H_0 + H_1(t)$ (with a suitable choice of modulation parameters) with an initial Gaussian wave packet whose width in k space is small compared to its typical length scale. The time evolution of the wave packet is then registered while the phase is linearly swept $\phi(t) = \gamma t$. The evolution of the mean position $\langle X\rangle(t)$ is shown in Fig. 3 (blue circles) and shows a good agreement with the analytical expression Eq. (17), validating our proposal.

IV. DISPERSION RELATIONS IN TWO DIMENSIONS

The strategy developed in Sec. II can be generalized to higher dimensions. We give here two examples: the creation of 2D Dirac points and of a Lieb lattice dispersion relation with a flat band.

A. Creating, moving, and the merging of Dirac cones

Manipulation of Dirac points both in optical lattices [20] and crystals [50] is an active research subject. A 2D optical lattice simulating Dirac physics was discussed in Ref. [22]. In brief, the corresponding dispersion relations can be synthesized in a 2D modulated tilted lattice. Hamiltonian (2) is easily translated into 2D (the definition of the dimensionless units is analogous to the 1D case):

$$H_{0_{2D}} = \frac{p_x^2+p_y^2}{2m^*} - V_0[\cos(2\pi x) + \cos(2\pi y)] + \omega_B^{(x)}x + \omega_B^{(y)}y. \quad (18)$$

Since the above Hamiltonian is separable, all Wannier-Stark properties described in Sec. II trivially generalize to the present case. We consider only *ground* ladder eigenstates formed by the tensorial product $\varphi_n^{(x)}(x)\varphi_m^{(y)}(y)$ with $\varphi_s^{(i)}(x_i) = \varphi_0^{(i)}(x_i - sx_{0_i})$, $i = \{x, y\}$, $s = \{n, m\}$ with eigenenergies $E_0 + n\omega_B^{(x)} + m\omega_B^{(y)}$.

The controlled dynamics for the Dirac system we are interested in is generated by adding a perturbation

$$H_{1_{2D}}(x,y,t) = \cos(\pi x)[V_x e^{i(2\omega_B^{(x)}t+\phi_x)} + \text{c.c.} + V_0] + [V_y \cos(2\pi y)e^{i(\omega_B^{(y)}t+\phi_y)} + \text{c.c.}], \quad (19)$$

depending on the arbitrary phases $\phi_{x,y}$. The general solution (restricted to the ground ladder) can be written, in analogy with Eq. (4),

$$\Psi(x,y,t) = \sum_{n,m} c_{n,m}(t)\varphi_n^{(x)}(x)\varphi_m^{(y)}(y). \quad (20)$$

Substituting the above solution in Schrödinger's equation for the total Hamiltonian $H_{0_{2D}} + H_{1_{2D}}$, one obtains the following set of coupled equations (in the resonant approximation):

$$i\frac{dc_{n,m}}{dt} = (-1)^n[T_x e^{i\phi_x}c_{n+2,m} + T_x e^{-i\phi_x}c_{n-2,m} + T_0 c_{n,m}] + T_y e^{i\phi_y}c_{n,m+1} + T_y e^{-i\phi_y}c_{n,m-1}$$

with couplings

$$T_x = V_x\langle\varphi_0^{(x)}|\cos(\pi x)|\varphi_2^{(x)}\rangle$$
$$T_y = V_y\langle\varphi_0^{(y)}|\cos(2\pi y)|\varphi_1^{(y)}\rangle$$
$$T_0 = V_0\langle\varphi_0^{(x)}|\cos(\pi x)|\varphi_0^{(x)}\rangle,$$

where the factor $\cos(\pi x)$ in Eq. (19) introduces a parity-dependent factor $(-1)^n$ which results in a system of two coupled sublattices corresponding to sites where n is odd or even. In the reciprocal space (k_x, k_y), we define two-dimensional Fourier amplitudes,

$$\tilde{c}(k_x,k_y,t) = \sum_{n\text{ even}}\sum_m c_{nm}(t)e^{-ink_x}e^{-imk_y},$$

for n even and, equivalently, for n odd, $\tilde{d}(k_x,k_y,t)$. These amplitudes can be written as a two-component spinor $[\psi] = (\tilde{c}(k_x,k_y,t), \tilde{d}(k_x,k_y,t))^{\mathsf{T}}$. The Hamiltonian projected in the k space turns out to be

$$\begin{bmatrix} T_0 + T_x\cos(2k_x+\phi_x) & T_y\cos(k_y+\phi_y) \\ T_y\cos(k_y+\phi_y) & -T_0 - T_x\cos(2k_x+\phi_x)\end{bmatrix}, \quad (21)$$

for which the dispersion relation is

$$\omega(k_x,k_y) = \pm\{[T_0 + T_x\cos(2k_x+\phi_x)]^2 + [T_y\cos(k_y+\phi_y)]^2\}^{1/2}. \quad (22)$$

In the $k_{x,y} \to 0$ limit, choosing $\phi_x = \phi_y = \pi/2$ and $T_0 = 0$, a Dirac equation (for a free particle) is obtained with the dispersion relation

$$\omega(k_x,k_y) = \pm\sqrt{4T_x^2k_x^2 + T_y^2k_y^2},$$

which is a Dirac cone (anisotropic if $2T_x \neq T_y$).

Another interesting situation is obtained from Eq. (22) with $\phi_x = 0$, $\phi_y = \pi/2$, and $T_0 \neq 0$. Then the dispersion relation is, for small k_y,

$$\omega(k_x,k_y) \approx \pm\sqrt{[T_0 + T_x\cos(2k_x)]^2 + T_y^2k_y^2}. \quad (23)$$

Depending on parameters T_0 and T_x, different structures are obtained (assuming here T_0 and T_x of opposite sign without loss of generality). As shown in Fig. 4, when $|T_0| < |T_x|$, there are two Dirac cones centered at the positions $k_y = 0$ and $k_x = \pm(1/2)\cos^{-1}(|T_0/T_x|)$. These cones move towards each other as the value of $|T_0/T_x|$ increases and finally coalesce when $T_0 = -T_x$, giving a dispersion relation $\omega(k_x,k_y) \approx \pm\sqrt{4T_x^2k_x^4 + T_y^2k_y^2}$ in the vicinity of the point $k_x, k_y = 0$, which is thus a hybrid point with a linear dependence in the y direction (corresponding to a free Dirac particle, or phonon) and quadratic dependence in x (corresponding to a free nonrelativistic particle). A gap opens for $|T_0| > |T_x|$, potentially leading to topological effects.

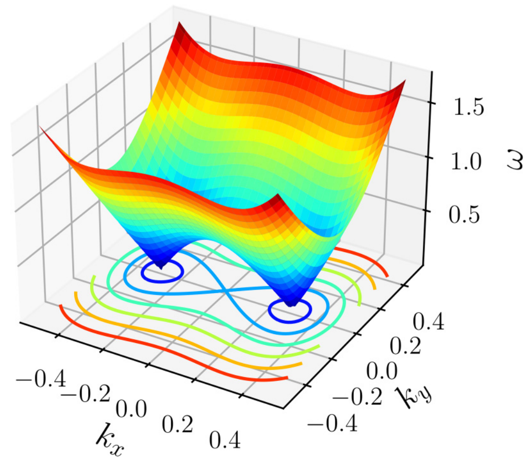

FIG. 4. Dirac cones. We plot the positive root of Eq. (23) for parameters: $T_x = T_y = 3$ and $T_0 = -2.5$ with two Dirac points.

B. The Lieb lattice

In this section we consider the synthesis of a Lieb lattice dispersion relation [5–7] using a form of Eq. (19) which results in an effective spin $S = 1$ with a flat band. The idea is sketched in Fig. 5, essentially consisting in creating different types of sites: A, B, coupled with coupling T_x; B and C

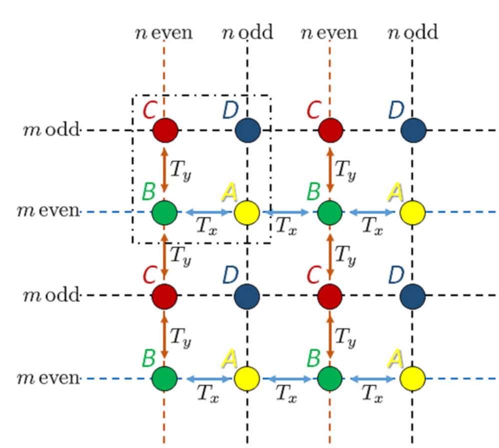

FIG. 5. Synthesis of a Lieb lattice. The unit cell is indicated by the dashed-dotted square. Sites D (n and m odd) are uncoupled to their neighbors. The other sites A, B, and C are resonantly coupled to their neighbors: B to C with amplitude T_y along the lines of m even; A to B with amplitude T_x along the lines of n even.

coupled with T_y; while sites D are completely uncoupled and thus dynamically irrelevant. This selective coupling can be obtained with the following perturbation:

$$H_{1_{2D}}(x,y,t) = \cos(2\pi x)\big[V_x^{(1)} + V_x^{(2)}\cos(\pi y)\big]\cos\big(\omega_B^{(x)}t\big) + \cos(2\pi y)\big[V_y^{(1)} + V_y^{(2)}\cos(\pi x)\big]\cos\big(\omega_B^{(y)}t\big).$$

By substituting the general solution, Eq. (20), in Schrödinger's equation for the Hamiltonian $H_{0_{2D}} + H_{1_{2D}}$ one obtains the following set of coupled equations (in the resonant approximation):

$$i\frac{dc_{n,m}}{dt} = T_x[1 + (-1)^m](c_{n+1,m} + c_{n-1,m}) + T_y[1 + (-1)^n](c_{n,m+1} + c_{n,m-1}) \qquad (24)$$

with couplings

$$T_x = \tfrac{1}{2}V_x^{(1)}\big\langle\varphi_0^{(x)}\big|\cos(2\pi x)\big|\varphi_1^{(x)}\big\rangle$$
$$T_y = \tfrac{1}{2}V_y^{(1)}\big\langle\varphi_0^{(y)}\big|\cos(2\pi y)\big|\varphi_1^{(y)}\big\rangle,$$

provided that the modulation amplitudes obey the following relations:

$$V_x^{(1)} = V_x^{(2)}\big\langle\varphi_0^{(y)}\big|\cos(\pi y)\big|\varphi^{(y)}\big\rangle$$
$$V_y^{(1)} = V_y^{(2)}\big\langle\varphi_0^{(x)}\big|\cos(\pi x)\big|\varphi^{(x)}\big\rangle.$$

As expected, Eq. (24) shows that the complex amplitudes $c_{n,m}$ with n and m odd (corresponding to D sites) are dynamically inert. These amplitudes are therefore irrelevant and, as shown in Fig. 5, the effective unit cell contains only three relevant sites, which is the characteristic of Lieb lattices.

In the same spirit as in Sec. IV A we define three amplitudes in k space:

$$\tilde{c}(k_x,k_y,t) = \sum_{n\text{ even}}\sum_{m\text{ even}} c_{nm}(t)e^{-ink_x}e^{-imk_y},$$

and $\tilde{d}(k_x,k_y,t)$ for m even, n odd, and $\tilde{f}(k_x,k_y,t)$ for m odd, n even. The time evolution in k-space for the three-component spinor $[\psi] = (\tilde{c}(k_x,k_y,t), \tilde{d}(k_x,k_y,t), \tilde{f}(k_x,k_y,t))^{\mathsf{T}}$ obeys

$$i\frac{d[\psi]}{dt} = \begin{bmatrix} 0 & 4T_y\cos k_y & 4T_x\cos k_x \\ 4T_y\cos k_y & 0 & 0 \\ 4T_x\cos k_x & 0 & 0 \end{bmatrix}[\psi],$$

leading to the well-known three-band dispersion relation of the Lieb lattice:

$$\omega(k_x,k_y) = 0$$
$$\omega(k_x,k_y) = \pm\sqrt{(4T_x\cos k_x)^2 + (4T_y\cos k_y)^2}, \qquad (25)$$

where the first expression corresponds to the flat band and the second one to two symmetric bands, which are anisotropic if $T_x \neq T_y$, as shown in Fig. 6.

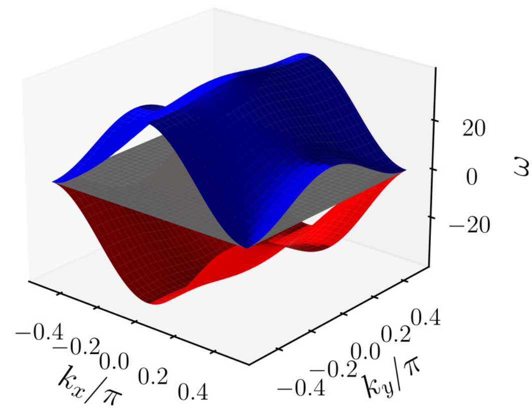

FIG. 6. Lieb lattice dispersion relation, Eq. (25). Parameters are $T_x = 1.5$, $T_y = 1$.

V. CONCLUSION

We introduced in this work a technique allowing the generation of a variety of dispersion relations in a tilted modulated lattice, which we illustrated through several important examples: the 1D Dirac phononic dispersion relation, the Bogoliubov dispersion relation, and the Landau superfluid relation, with the maxon and the roton features. We proposed a simple way to experimentally detect the dispersion relation by adding a slow phase shift to the modulation and measuring an easily accessible quantity, namely, the average position of the wave packet. Finally, we illustrated the generation of Dirac points in two dimensions and the generation of a flat band in a Lieb lattice. The technique introduced in the present work thus appears as an efficient, state-of-the-art experimentally feasible way to synthesize lattice systems with arbitrary dispersion relations, thus mimicking several important condensed matter systems.

ACKNOWLEDGMENTS

This work was supported by Agence Nationale de la Recherche through the MANYLOK project (Grant No. ANR-18-CE30-0017), the Labex CEMPI (Grant No. ANR-11-LABX-0007-01), the Ministry of Higher Education and Research, Hauts-de-France Council, and European Regional Development Fund (ERDF) through the Contrat de Projets État-Région (CPER Photonics for Society, P4S).

APPENDIX: DYNAMICS IN A PHASE-MODULATED LATTICE

In this Appendix we show how the introduction of a phase shift allows to extract the shape of the dispersion relation from the measurement of the average wave-packet position evolution.

Consider a smooth wave packet in a system obeying a dispersion relation $\omega(k,t)$. Its average position $\langle X\rangle(t)$ can be written as

$$\langle X\rangle(t) = \langle X\rangle(t=0) + \int_0^t v_G(t')dt',$$

where $v_G(t) = d\omega/dk$ is the group velocity.

An adiabatic phase shift $\varphi(t) = \gamma t$ corresponds to $k(t) = k_0 + \gamma t$, and thus, by integration,

$$\langle X\rangle(t) = \langle X\rangle(t=0) + [\omega(k(t)) - \omega(k_0)]/\gamma,$$

with $\langle X\rangle(t=0)=0$. Choosing k_0 such that $\omega(k_0)=0$ results in the simple expression

$$\langle X\rangle(t)=\omega(k(t))/\gamma.$$

Hence, measuring the temporal evolution of the average position of the wave packet directly gives the shape of the dispersion relation.

[1] L. Landau, Theory of the superfluidity of helium II, Phys. Rev. **60**, 356 (1941).

[2] A. Leggett, *Quantum Liquids: Bose Condensation and Cooper Pairing in Condensed-Matter Systems* (Oxford Science Publications, Oxford, UK, 2006).

[3] C. Barenghi and N. G. Parker, *A Primer on Quantum Fluids* (Springer, Heidelberg, 2016).

[4] G.-B. Jo, J. Guzman, C. K. Thomas, P. Hosur, A. Vishwanath, and D. M. Stamper-Kurn, Ultracold Atoms in a Tunable Optical Kagome Lattice, Phys. Rev. Lett. **108**, 045305 (2012).

[5] M. R. Slot, T. S. Gardenier, P. H. Jacobse, G. C. P. van Miert, S. N. Kempkes, S. J. M. Zevenhuizen, C. M. Smith, D. Vanmaekelbergh, and I. Swart, Experimental realization and characterization of an electronic Lieb lattice, Nat. Phys. **13**, 672 (2017).

[6] N. Goldman, D. F. Urban, and D. Bercioux, Topological phases for fermionic cold atoms on the Lieb lattice, Phys. Rev. A **83**, 063601 (2011).

[7] S. Flannigan, L. Madail, R. G. Dias, and A. J. Daley, Hubbard models and state preparation in an optical Lieb lattice, New J. Phys. **23**, 083014 (2021).

[8] G. Roati, C. d'Errico, L. Fallani, M. Fattori, C. Fort, M. Zaccanti, G. Modugno, M. Modugno, and M. Inguscio, Anderson localization of a non-interacting Bose-Einstein condensate, Nature (London) **453**, 895 (2008).

[9] J. Billy, V. Josse, Z. Zuo, A. Bernard, B. Hambrecht, P. Lugan, D. Clément, L. Sanchez-Palencia, P. Bouyer, and A. Aspect, Direct observation of Anderson localization of matter-waves in a controlled disorder, Nature (London) **453**, 891 (2008).

[10] F. L. Moore, J. C. Robinson, C. Bharucha, P. E. Williams, and M. G. Raizen, Observation of Dynamical Localization in Atomic Momentum Transfer: A New Testing Ground for Quantum Chaos, Phys. Rev. Lett. **73**, 2974 (1994).

[11] M. Ben Dahan, E. Peik, J. Reichel, Y. Castin, and C. Salomon, Bloch Oscillations of Atoms in an Optical Potential, Phys. Rev. Lett. **76**, 4508 (1996).

[12] S. R. Wilkinson, C. F. Bharucha, K. W. Madison, Q. Niu, and M. G. Raizen, Observation of Atomic Wannier-Stark Ladders in an Accelerating Optical Potential, Phys. Rev. Lett. **76**, 4512 (1996).

[13] D. Jaksch, C. Bruder, J. I. Cirac, C. W. Gardiner, and P. Zoller, Cold Bosonic Atoms in Optical Lattices, Phys. Rev. Lett. **81**, 3108 (1998).

[14] M. Greiner, O. Mandel, T. Esslinger, T. W. Hänsch, and I. Bloch, Quantum phase transition from a superfluid to a Mott insulator in a gas of ultracold atoms, Nature (London) **415**, 39 (2002).

[15] F. Trimborn, D. Witthaut, and H. J. Korsch, Beyond mean-field dynamics of small Bose-Hubbard systems based on the number-conserving phase-space approach, Phys. Rev. A **79**, 013608 (2009).

[16] F. L. Moore, J. C. Robinson, C. F. Bharucha, B. Sundaram, and M. G. Raizen, Atom Optics Realization of the Quantum Rotor, Phys. Rev. Lett. **75**, 4598 (1995).

[17] J. Chabé, G. Lemarié, B. Grémaud, D. Delande, P. Szriftgiser, and J. C. Garreau, Experimental Observation of the Anderson Metal-Insulator Transition with Atomic Matter Waves, Phys. Rev. Lett. **101**, 255702 (2008).

[18] R. Gerritsma, G. Kirchmair, F. Zahringer, E. Solano, R. Blatt, and C. F. Roos, Quantum simulation of the Dirac equation, Nature (London) **463**, 68 (2010).

[19] D. Witthaut, T. Salger, S. Kling, C. Grossert, and M. Weitz, Effective Dirac dynamics of ultracold atoms in bichromatic optical lattices, Phys. Rev. A **84**, 033601 (2011).

[20] L. Tarruell, D. Greif, T. Uehlinger, G. Jotzu, and T. Esslinger, Creating, moving and merging Dirac points with a Fermi gas in a tunable honeycomb lattice, Nature (London) **483**, 302 (2012).

[21] J. C. Garreau and V. Zehnlé, Simulating Dirac models with ultracold atoms in optical lattices, Phys. Rev. A **96**, 043627 (2017).

[22] J. C. Garreau and V. Zehnlé, Analog quantum simulation of the spinor-four Dirac equation with an artificial gauge field, Phys. Rev. A **101**, 053608 (2020).

[23] S. S. Kondov, W. R. McGehee, J. J. Zirbel, and B. DeMarco, Three-dimensional Anderson localization of ultracold matter, Science **334**, 66 (2011).

[24] F. Jendrzejewski, A. Bernard, K. Müller, P. Cheinet, V. Josse, M. Piraud, L. Pezzè, L. Sanchez-Palencia, A. Aspect, and P. Bouyer, Three-dimensional localization of ultracold atoms in an optical disordered potential, Nat. Phys. **8**, 398 (2012).

[25] G. Semeghini, M. Landini, P. Castilho, S. Roy, G. Spagnolli, A. Trenkwalder, M. Fattori, M. Inguscio, and G. Modugno, Measurement of the mobility edge for 3D Anderson localization, Nat. Phys. **11**, 554 (2015).

[26] R. Gerritsma, B. P. Lanyon, G. Kirchmair, F. Zähringer, C. Hempel, J. Casanova, J. J. García-Ripoll, E. Solano, R. Blatt, and C. F. Roos, Quantum Simulation of the Klein Paradox with Trapped Ions, Phys. Rev. Lett. **106**, 060503 (2011).

[27] D. Suchet, M. Rabinovic, T. Reimann, N. Kretschmar, F. Sievers, C. Salomon, J. Lau, O. Goulko, C. Lobo, and F. Chevy, Analog simulation of Weyl particles with cold atoms, Europhys. Lett. **114**, 26005 (2016).

[28] D. H. Dunlap and V. M. Kenkre, Dynamic localization of a charged particle moving under the influence of an electric field, Phys. Rev. B **34**, 3625 (1986).

[29] E. N. Bulgakov and A. R. Kolovsky, Induced tunneling and localization for a quantum particle in tilted two-dimensional lattices, Phys. Rev. B **89**, 035116 (2014).

[30] A. R. Kolovsky, Topological phase transitions in tilted optical lattices, Phys. Rev. A **98**, 013603 (2018).

[31] C. Cohen-Tannoudji and D. Guéry-Odelin, *Advances In Atomic Physics: An Overview* (World Scientific Publishing, Singapore, 2011).

[32] We use a sans serif font for dimensioned quantities, except when no confusion is possible (e.g., λ_L).

[33] I. Manai, J.-F. Clément, R. Chicireanu, C. Hainaut, J. C. Garreau, P. Szriftgiser, and D. Delande, Experimental Observation of Two-Dimensional Anderson Localization with the Atomic Kicked Rotor, Phys. Rev. Lett. **115**, 240603 (2015).

[34] The force can be generated by applying a linear chirp to one of the beams forming the standing wave so that the nodes of the resulting standing wave are uniformly accelerated. In the (noninertial) reference frame where the standing wave is at rest, the atoms feel a constant inertial force.

[35] G. H. Wannier, The structure of electronic excitation levels in insulating crystals, Phys. Rev. **52**, 191 (1937).

[36] M. Glück, A. R. Kolovsky, and H. J. Korsch, Lifetime of Wannier-Stark States, Phys. Rev. Lett. **83**, 891 (1999).

[37] M. Glück, M. Hankel, A. R. Kolovsky, and H. J. Korsch, Wannier-Stark ladders in driven optical lattices, Phys. Rev. A **61**, 061402(R) (2000).

[38] H. L. Haroutyunyan and G. Nienhuis, Coherent control of atom dynamics in an optical lattice, Phys. Rev. A **64**, 033424 (2001).

[39] Q. Thommen, J. C. Garreau, and V. Zehnlé, Theoretical analysis of quantum dynamics in one-dimensional lattices: Wannier-Stark description, Phys. Rev. A **65**, 053406 (2002).

[40] M. Glück, A. R. Kolovsky, and H. J. Korsch, Wannier-Stark resonances in optical and semiconductor superlattices, Phys. Rep. **366**, 103 (2002).

[41] P. Plötz, P. Schlagheck, and S. Wimberger, Effective spin model for interband transport in a Wannier-Stark lattice system, Eur. Phys. J. D **63**, 47 (2021).

[42] The translation symmetry $\varphi_n^{(\ell)}(x - na) = \varphi_0^{(\ell)}(x)$ implies $\langle\varphi_n^{(\ell)}|V|\varphi_{n+r}^{(\ell)}\rangle = \langle\varphi_0^{(\ell)}|V|\varphi_r^{(\ell)}\rangle$ for $V = \cos(2\pi x)$.

[43] C. J. Pethick and H. Smith, *Bose-Einstein Condensation in Dilute Gases*, 2nd ed. (Cambridge University Press, Cambridge, UK, 2008).

[44] The roton minimum determines Landau's critical velocity given by slope of the dispersion relation, thus setting a gap responsible for the superfluidity.

[45] L.-C. Ha, L. W. Clark, C. V. Parker, B. M. Anderson, and C. Chin, Roton-Maxon Excitation Spectrum of Bose Condensates in a Shaken Optical Lattice, Phys. Rev. Lett. **114**, 055301 (2015).

[46] L. Chomaz, R. M. W. van Bijnen, D. Petter, G. Faraoni, S. Baier, J. H. Becher, M. J. Mark, F. Wächtler, L. Santos, and F. Ferlaino, Observation of roton mode population in a dipolar quantum gas, Nat. Phys. **14**, 442 (2018).

[47] L. Santos, G. V. Shlyapnikov, and M. Lewenstein, Roton-Maxon Spectrum and Stability of Trapped Dipolar Bose-Einstein Condensates, Phys. Rev. Lett. **90**, 250403 (2003).

[48] Y. Chen, M. Kadic, and M. Wegener, Roton-like acoustical dispersion relations in 3D metamaterials, Nat. Commun. **12**, 3278 (2021).

[49] That is, ϕ acts as a (time-dependent) quasimomentum.

[50] G. Montambaux, F. Piéchon, J.-N. Fuchs, and M. O. Goerbig, Merging of Dirac points in a two-dimensional crystal, Phys. Rev. B **80**, 153412 (2009).